Machine learning maximized Anderson localization of phonons in aperiodic superlattices

Prabudhya Roy Chowdhury [a], Colleen Reynolds [b,1], Adam Garrett [a], Tianli Feng [c], Shashishekar P. Adiga [b,**,2], Xiulin Ruan [a,*]

[a] School of Mechanical Engineering and the Birck Nanotechnology Center, Purdue University, West Lafayette, IN, 47907-2088, USA
[b] Lockheed Martin Advanced Technology Laboratories, 3, Executive Campus, Cherry Hill, NJ, 08002, USA
[c] Building Technologies Research and Integration Center, Energy and Transportation Science Division, Oak Ridge National Laboratory, Oak Ridge, TN, 37831, USA

ARTICLE INFO

ABSTRACT

Nanostructuring materials to achieve ultra-low lattice thermal conductivity has proven to be extremely attractive for numerous applications such as thermoelectric energy conversion. Anderson localization of phonons due to aperiodicity can reduce thermal conductivity in superlattices, but the lower limit of thermal conductivity remains elusive due to the prohibitively large design space. In this work, we demonstrate that an intuition-based manual search for aperiodic superlattice structures (random multilayers or RMLs) with the lowest thermal conductivity yields only a local minimum, while a genetic algorithm (GA) based approach can efficiently identify the globally minimum thermal conductivity by only exploring a small fraction of the design space. Our results show that this minimum value occurs at an average RML period that is, surprisingly, smaller than the period corresponding to the minimum SL thermal conductivity. Above this critical period, scattering of incoherent phonons at interfaces is less, whereas below this period, the room for randomization becomes less, thus putting more coherent phonons out of Anderson localization and causing increased thermal conductivity. Moreover, the lower limit of the thermal conductivity occurs at a moderate rather than maximum randomness of the layer thickness. Our machine learning approach demonstrates a general process of exploring an otherwise prohibitively large design space to gain non-intuitive physical insights.

1. Introduction

The design and discovery of nanostructured materials with targeted thermal transport properties has become increasingly important in various applications such as thermal management of electronic chips and batteries [1,2], thermal interface materials [3,4], thermal barrier coatings [5,6] and thermoelectrics [7]. For example, high figure-of-merit thermoelectric devices require ultra-low thermal conductivity materials without significantly reduced electrical conductivity. Several methods have been investigated to reduce thermal conductivity by increasing phonon scattering using isotopes [8,9], defects [10,11] and grain boundaries [12]. In the past few decades, multilayer phononic structures such as binary superlattices (SLs) have gained widespread attention due to their potential for low thermal conductivity caused by increased interface scattering [13–16]. The thermal conductivity of SLs exhibits a minimum with variation of superlattice period, which has been observed in many numerical studies [17–21] and confirmed in some experimental investigations [13,22–25].

Recently, it has been predicted that the minimum thermal conductivity can be further suppressed by randomizing the SL layer thicknesses [26–29], which introduces phase-preserving scattering mechanisms leading to coherent phonon localization. Wang et al. [27] formulated a two-phonon model to decompose the thermal conductivity of SLs and RMLs into coherent and incoherent phonon contributions. Moreover, the influence of parameters such as bond strength [28], interface roughness [28,30,31] and isotopic modulation [32] on the thermal conductivity of multilayer structures has also been investigated. More recently, evidence of localization of coherent phonons in disordered

graphene phononic crystals was shown by Hu et al. [33], while Juntunen et al. [34] provided a spectral description of the frequency-dependent phonon localization lengths in Si/Ge RML systems. We note that in many of the above studies, the variation in thermal conductivities of RMLs arising from independently generated random structures was not elucidated. In contrast, Ju et al. [35] observed a significant spread in thermal conductivities of Si/Ge RMLs with different distributions of layer thickness, even at the same average period and composition ratio. Their results indicate that such structural parameters give rise to a very large design space, yet their effect on the lower limit of RML thermal conductivity has not been resolved. An optimization study within this design space will enable us to obtain a more fine-grained tunability of thermal conductivity as well as gain insight into the underlying physics of phonon transport in RML structures.

The selection of experiments and simulations for materials discovery and property engineering has traditionally been guided by the domain knowledge of researchers in the relevant field. However, such intuition-based explorations, combined with prohibitively large design spaces, may preclude the discovery of low-probability-of-occurrence novel solutions which show counter-intuitive trends. Recently, metaheuristics and machine learning-based methods have increasingly been used to accelerate the exploration of new materials with targeted properties [36, 37], prediction of material structures [38,39] and optimization of nanostructure geometry [35,40,41]. The availability of specialized hardware architectures has led to increased popularity of various machine learning techniques including neural networks [42–44], genetic algorithms [45,46] and support vector machines [47] among others. In this work, we use a genetic algorithm (GA)-based search process in conjunction with molecular dynamics (MD) simulations to discover the lower limit of thermal conductivity in Si/Ge random multilayer systems. Our machine learning based approach demonstrates the elimination of human bias in the search process, thereby allowing us to identify non-intuitive trends in structural features leading to ultralow thermal conductivity. It is observed that the minimum RML thermal conductivity occurs, surprisingly, at a lower average period than that at which the minimum superlattice thermal conductivity is found. Finally, it is desirable, but challenging, to come up with a set of descriptors out of the optimization process, which can be intuitively understood and adopted during experimental realizations of such systems. Our work provides a hierarchical description of these structural features that will provide guidance for application of RML systems in various applications.

2. Simulation methods

2.1. Designing RML structures

We have studied superlattice (SL) and random multilayer (RML) structures created from diamond structured Si and Ge with the heat transport along the [001] direction. A number of theoretical and numerical studies have been performed on Si/Ge systems such as bulk alloys [48,49], superlattice thin films [50–53] and superlattice nanowires [54–56], due to the ubiquitous presence of these semiconductors in a variety of applications. The lattice constant is initially set at 0.543 nm which is the room temperature lattice constant of silicon. To create the SL and RML structures, layers of Si and Ge are stacked along the [001] direction in a periodic and random manner, respectively. The smallest allowable thickness of a layer is chosen to be one unit cell. The representative SL and RML structures are shown in Fig. 1(a–b). The period of the SL is defined as the total thickness of a pair of consecutive Si and Ge layers, while for the RML, the period is calculated as the sum of the average thicknesses of Si and Ge layers in the whole structure. We perform our calculations for system sizes of 6×6 unit cells in the in-plane direction (cross-section), and 40 unit cells (21.72 nm) in the cross-plane direction. No constraint is placed on the composition ratio of the RML structures (ratio of the number of layers of Si and Ge), which is allowed to vary during the optimization procedure.
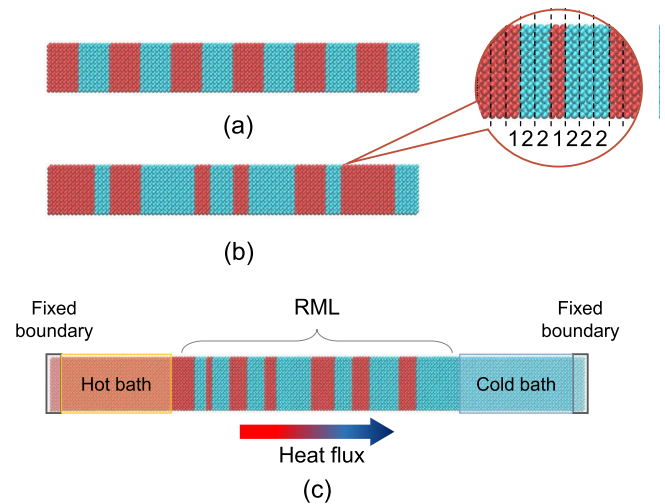

Fig. 1. Representative structures showing (a) superlattice of period 4.4 nm and (b) random multilayer with the same average period. Inset shows encoding of the RML structure in the GA as an *N*-bit array, where each bit is assigned 1 or 2 if the unit cell is Si or Ge respectively. (c) Schematic of the NEMD simulation setup showing the RML sandwiched between two heat baths which are thermostatted to impose a heat flux through the system.

2.2. Non-equilibrium molecular dynamics simulations

Non-equilibrium molecular dynamics (NEMD) simulations are performed using LAMMPS [57] to calculate the thermal conductivity of the multilayer structures. The schematic of the simulation setup is shown in Fig. 1 (c). The SL/RML is placed between two heat bath regions on either side which are capped by two end regions of fixed atoms to prevent sublimation. The interaction between Si and Ge atoms is modeled using the Tersoff potential [58], which has been widely used to predict thermal transport in Si–Ge system. The equations of motion are integrated using a Verlet algorithm with a timestep of 0.5 fs. Initially, periodic boundary conditions are applied in all directions and the system is relaxed at zero pressure and a temperature of 300 K in an NPT ensemble for 500 ps, after which it is run for another 250 ps in an NVE ensemble to observe proper conservation of energy. To introduce non-equilibrium conditions, the atoms in the two end regions are then fixed, and the temperatures of the hot and cold baths are maintained at 330 K and 270 K respectively using Langevin thermostats to create a temperature gradient in the multilayer region. The system is allowed to reach steady state over a time of 4.5 ns and the temperature profile is monitored by binning the velocities of atoms along the direction of heat transport. The cross-plane thermal conductivity is then obtained from the steady state heat flux q'' as

$$\kappa = \frac{q''}{\Delta T/L} \tag{1}$$

where L is the length of the multilayer structure. The thermal boundary resistance (TBR) is calculated from the temperature drop at each individual interface (ΔT_i) as

$$R_i = \frac{\Delta T_i}{q''} \tag{2}$$

2.3. Genetic algorithm based optimization method

Genetic algorithms are a class of evolutionary algorithms which mimic the principle of natural selection to arrive at the optimal solution. The basic principle used by a GA is that already identified good solutions in one iteration can lead to potentially better solutions in the next iteration through evolutionary operations. In a GA based optimization,

each candidate solution in a multivariate design space is represented by a string called a *chromosome*, formed by concatenating the individual variables encoded using *genes*. A commonly used approach to perform this encoding is to convert numeric values into binary strings, which lend themselves conveniently to evolutionary operations. In the initial iteration, a population is formed out of a chosen number of chromosomes, which may be generated randomly or using previous knowledge about the design space. An objective function is designed for the particular problem to evaluate the performance of candidate solutions. Each member of the initial population is assigned a fitness value equal to the corresponding value of the objective function. Subsequently, a new population of the same number of chromosomes is generated by performing the evolutionary operations of selection, crossover and mutation on the individuals of the current population. Selection is performed by choosing individuals with high fitness values to propagate to the next iteration, and ensures that only the best individuals in the current iteration are carried over to the next. Crossover (or reproduction) produces new candidate solutions by combining genes from the selected individuals to produce new chromosomes, while mutation perturbs the value of randomly selected genes within a chromosome to generate individuals belonging to unexplored areas of the design space. Crossover and mutation are performed probabilistically by specifying rates of occurrence of the operations. This is usually done by generating a random number between 0 and 1 and performing the operation if the generated number is below the probability rate of the corresponding process. Together, the crossover and mutation operators ensure that the search does not get trapped in a local optimum within the solution space. The GA progresses by performing the above operations on the new population members, until a convergence criteria is reached, which can be set with respect to the change in fitness value over successive generations.

We now discuss the implementation of the above steps in our GA based optimization process. To encode RML structures as chromosomes, an N-bit binary array is used for an RML of N unit cells length in the cross-plane direction. As shown in the inset of Fig. 1, each position in the array is coded as 1 if it is a Si unit cell and 2 if it is a Ge unit cell. Thus, each chromosome representing an RML structure is formed of N binary variables which can take values of 1 or 2. Additionally, the first and last unit cells which are in contact with the heat baths at each end are fixed to be Si (1) and Ge (2) respectively. As a result, the number of possible solutions in the design space is 2^{N-2}. A population size of 20 is used and the initial population is generated randomly or according to our choice for specific runs. The inverse of the cross-plane thermal conductivity is chosen as the objective function, which is maximum for the structure with the lowest thermal conductivity. To implement the selection process, we employ a rank-based selection scheme. In this scheme, the individuals are first sorted by fitness values from best to worst. The probability of each individual being selected for the next iteration is then proportional to the inverse of its rank. For every two individuals selected, crossover is performed to generate two new individuals. We use a single-point crossover, in which a position along the N-bit array is chosen randomly and the sections of the chromosome following this position are interchanged among the two parent chromosomes. In contrast, mutation involves a single chromosome and is implemented probabilistically in either of two ways: (i) at a single position randomly chosen along the chromosome, the value of the gene is flipped (1–2 or vice-versa), or (ii) a section of the N bit array with contiguous variables having the same value (1 or 2) is identified, and a few adjacent variables are then switched to the same value. The first process is found to have more influence on controlling the number of interfaces in the RML structure, whereas the second process primarily changes the average period and composition ratio by changing the thickness of a layer of Si or Ge. A schematic process flow of the GA based optimization process, involving evaluation of the fitness function and implementation of the crossover and mutation operations, is shown in Fig. 2.

The convergence of the GA based search process depends on the hyperparameters which must be carefully chosen to ensure a balance is achieved between exploration and exploitation of the design space. In this work, we use a trial-and-error based approach to arrive at suitable parameter values. The number of individuals in the population is chosen as 20 to keep the computational cost at each iteration low while still ensuring adequate sampling of the design space. We use a crossover probability of 0.8 and a mutation probability of 0.4 based on convergence rates observed in preliminary trials. The convergence criterion of the GA is met when the lowest thermal conductivity value does not change over several successive iterations.

3. Results and discussions

3.1. Manual intuition-based search for the minimum RML thermal conductivity

The thermal conductivities of the $N - N$ superlattice system of length 40 unit cells are first calculated, where $N = 1, 2, 4, 5, 10$ and 20 to allow only an integral number of periods. Fig. 3 (a) shows that a minimum superlattice thermal conductivity of around 3.5 W/mK is found to occur at period of 4.43 nm. The nature of the variation of thermal conductivity with average SL period has been explored in literature in significant detail [13,17–25]. The existence of the minimum superlattice thermal conductivity has been attributed to the competition between incoherent and coherent phonon dominated transport regimes. When the superlattice period $\bar{d}$ is large, phase breaking occurs due to anharmonic phonon-phonon scattering and the role of incoherent phonons become more important. As the superlattice period decreases, the increase in interface density leads to higher phonon-boundary scattering and reduced thermal conductivity. On the other hand, wave interference effects become increasingly important at small $\bar{d}$, and the phase breaking of phonons does not take place before the phonons scatter at the interfaces. The repeated reflections at periodic interfaces give rise to a modified phonon spectra including coherent phonon modes which are not scattered at the interfaces. Decreasing $\bar{d}$ below the critical superlattice period leads to an increase in thermal conductivity, which has been explained by effects such as less zone folding leading to weaker band flattening and increased group velocities.

The design space for imparting randomization to the superlattices is extremely high, making an exhaustive search for the RML with minimum thermal conductivity impossible. For a multilayer system consisting of N unit cells where the shortest layer length is constrained to be one unit cell, the total number of possible RML structures is 2^N. In such cases, the traditionally adopted best approach is to search a smaller subset of the solution space, guided by previously discovered knowledge and intuition about heat transport in multilayer structures. Since the superlattice thermal conductivity minimum is obtained around a period of 4 nm considering our results and those in literature [52], it can be intuitively expected that the RML with minimum thermal conductivity can be obtained by randomizing the layer thicknesses of the same superlattice. As a result, we perform a manual search by evaluating the thermal conductivities of 100 randomly generated RML structures with an average period of 4.43 nm. The thermal conductivities of such RML structures are plotted in Fig. 3 (a). The lowest thermal conductivity obtained among these structures is 2.45 W/mK for the structure shown in Fig. 3 (b), which represents a 30% reduction from the minimum superlattice thermal conductivity.

3.2. Genetic algorithm-based search for the minimum RML thermal conductivity

Considering the infeasibility of an exhaustive search of the extremely large solution space, the use of machine learning can benefit the current problem significantly. Here, we choose a genetic algorithm (GA) to predict the best simulations to perform on our finite computational
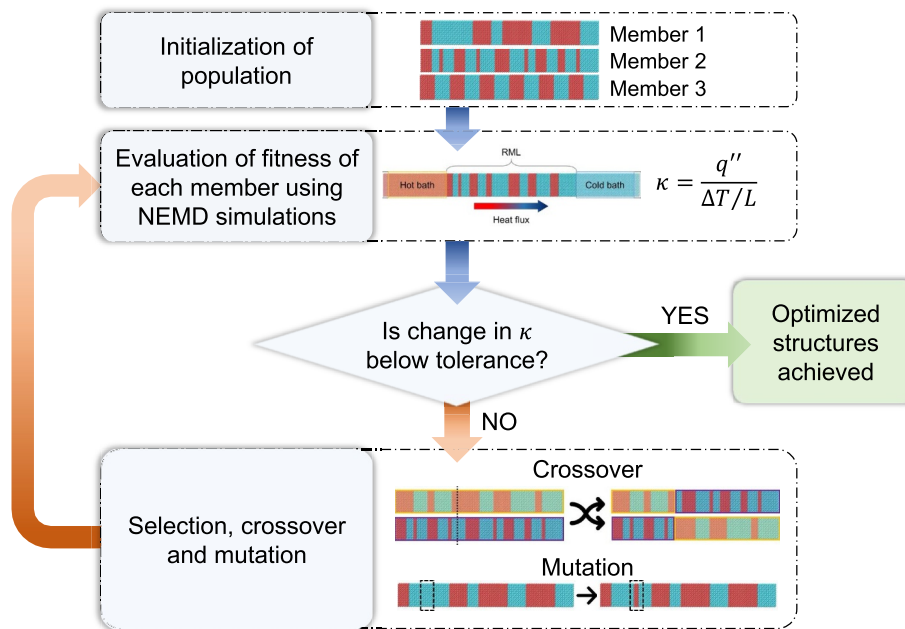
Fig. 2. Schematic of the genetic algorithm based optimization method showing the different steps involved. The GA population is initialized randomly with a chosen number of members and the fitness of each member is based on its thermal conductivity evaluated using NEMD simulations. The stopping criteria is checked and if it is not achieved, selection, crossover and mutation operations are carried out on the best individuals to obtain the next generation.
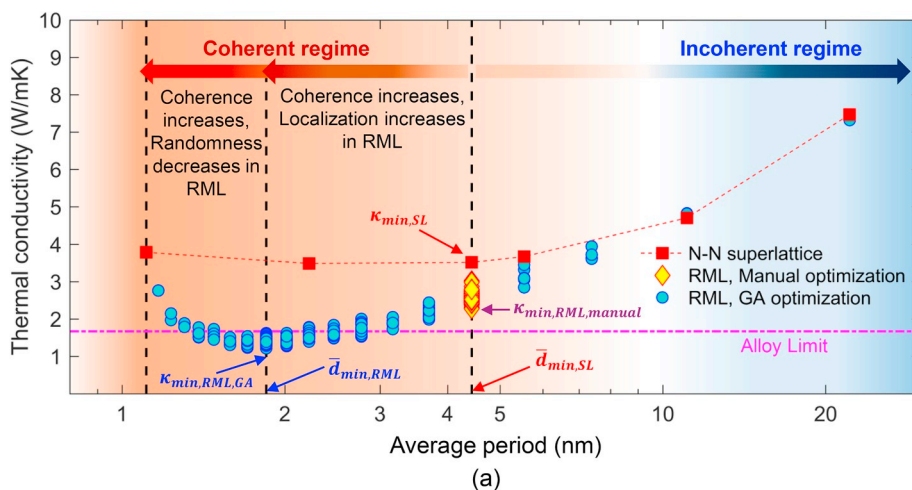

Fig. 3. (a) Variation of thermal conductivity with average period length for N–N superlattices (red squares), RML structures obtained using manual intuition-based optimization (diamonds) and RML structures obtained using machine-learning based optimization (filled circles). The minimum RML thermal conductivity obtained from our optimization algorithm occurs at a smaller average period than that at which the minimum superlattice thermal conductivity is observed. The dashed purple line marks the random alloy limit. (b) RML structure with minimum thermal conductivity obtained from a manual optimization, (c) RML structure with minimum thermal conductivity obtained from a machine-learning based optimization, and (d) RML structure with average period below $\bar{d}_{min,\,RML}$.
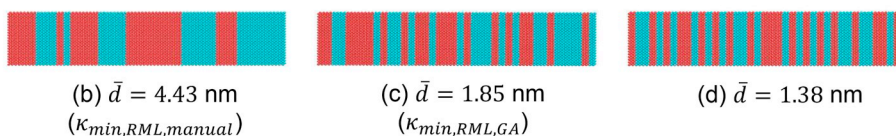
resources by utilizing information from the results of previously performed simulations. We apply the GA based search process on RML systems consisting of 40 unit cells (21.72 nm). In order to explore greater portions of the design space and avoid getting trapped within local minima, 15 independent GA runs are performed starting from different initial populations. Fig. 4 shows the results of one run started with an initial population consisting entirely of structures with a single Si–Ge interface and a composition ratio of 1. Since this structure has the lowest possible interface density, we expect it to be the worst candidate in the design space. As a result, this initial population can be considered as a starting point for the search when no prior knowledge or intuition is available about the minimum thermal conductivity. The genetic operators of crossover and mutation allow the GA to converge towards the

minimum thermal conductivity even with this sub-optimal initial population. The evolution of the population with iterations of the GA is shown in terms of thermal conductivity in Fig. 4 (a) and the average RML period in Fig. 4 (b). As seen in Fig. 4 (a), although all individuals of the initial population show high thermal conductivities, these gradually get eliminated from the population in subsequent generations. The reason for this can be understood by noting from Fig. 4 (b) that the later generations contain RMLs with much lower average periods and thus higher interface densities. The lowest thermal conductivity value for the entire population decreases rapidly and saturates about the minimum value in about 35 generations, in RMLs with an average period of 1.85 nm. The RML structure with the lowest thermal conductivity among all the GA searches performed is shown in Fig. 3 (c).
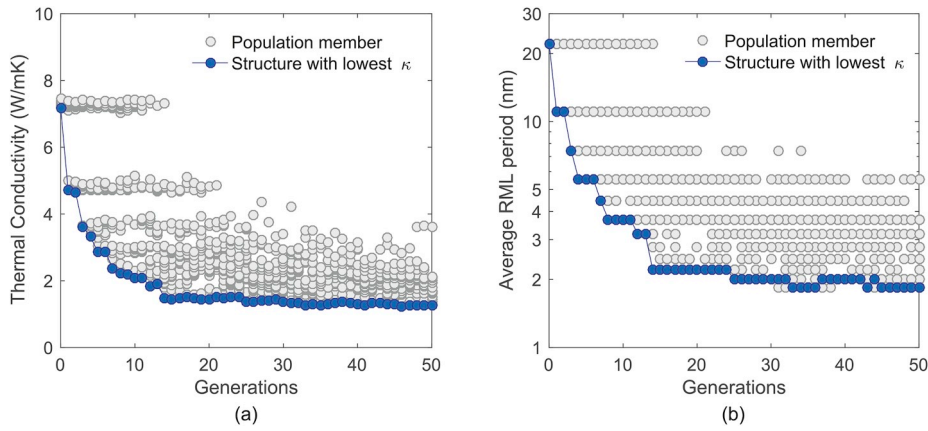
Fig. 4. Variation of (a) thermal conductivity and (b) average RML period of the population with each iteration of the genetic algorithm based search process. The blue circles mark the best individual (lowest κ) of each generation.

3.3. Influence of average RML period on the minimum thermal conductivity

To gain insight into our optimization results, the thermal conductivity variation with average period for the RMLs sampled during all our optimization runs on the 40 unit cell RML system is plotted in Fig. 3 (a). We only include structures with a composition ratio of 1 in order that the results can be compared to the $N - N$ superlattice system. The major transport regimes can be easily identified from the relative magnitudes of SL and RML thermal conductivities at different average periods. At high average RML periods (>10 nm), the thermal conductivity of RMLs is similar to that of SLs, indicating that randomization of layer thicknesses has negligible effect on thermal conductivity. Incoherent phonons, therefore, dominate thermal transport in both SLs and RMLs at these high periods. Below 10 nm, the thermal conductivity of RMLs keeps on decreasing with decreasing average period, while that of SL starts to level off. As a result, we can infer that coherent phonon transport starts becoming important in SLs in this region. As the average period further decreases, the thermal conductivity of the $N- N$ superlattice reaches a minimum at the critical SL period ($\bar{d}_{min,SL}$) and then bounces back. However, the thermal conductivities of RMLs keep on reducing until reaching a minimum at a period of $\bar{d}_{min,RML} = 1.85$ nm, which is, notably, much lower than the critical SL period ($\bar{d}_{min,SL}$). This surprising behaviour can be attributed to the fact that while the increasing phonon coherence leads to an increase in the thermal conductivity for the SL, it puts more phonon modes in localization in RMLs causing a decrease in thermal conductivity. Moreover, the occurrence of the observed minimum RML thermal conductivity at a smaller period than what was intuitively expected proves that our previous manual search could at best converge to a local minimum, and highlights the effectiveness of machine-learning based methods. We also calculated the random alloy limit of thermal conductivity by randomly assigning 50% of atomic masses in a Si structure of the same length to the mass of Ge, which is plotted in Fig. 3 (a). As seen from the figure, the GA-optimized RML structures are able to break the random alloy limit by more than 25%. Although the phonons in the random alloy structures have small mean free paths due to alloy scattering, they can still propagate and contribute to the thermal conductivity. However, the majority of coherent phonons in the RML are completely localized and have no contribution to the thermal transport, leading to lower thermal conductivity values.

Below $\bar{d}_{min,RML}$, the thermal conductivity of RMLs increases steeply as the average period decreases further. This occurs because at such low average periods, the room for randomizing the individual layer thicknesses from the periodic SL thickness becomes small, as a result of which localization of coherent phonons is reduced significantly. This is seen in

Fig. 3(b–d) where the RML with the lowest thermal conductivities obtained for three different average periods from the GA are plotted. For $\bar{d} = \bar{d}_{min,RML} = 1.85$nm (Fig. 3 (c)), the layer thicknesses have room to become sufficiently randomized to allow for localization of coherent phonons, while providing a high interface density for incoherent phonon scattering. The combination of both of these favourable effects leads to the existence of the minimum RML thermal conductivity at this period. For $\bar{d} = 1.38$nm $< \bar{d}_{min,RML}$ (Fig. 3 (d)), the majority of the superlattice has to be composed of single layers of Si and Ge arranged periodically, which allows for less room for localization of coherent phonons. In the limiting case of the shortest average period possible ($\bar{d} = 1$ unit cell of Si + 1 unit cell of Ge), the RML structure is the same as a 1-1 superlattice with no room for introducing randomness. On the other hand, at periods greater than $\bar{d}_{min,RML}$ (Fig. 3 (b)), the larger thicknesses of individual layers provide more freedom for randomization and spatial distribution of layers. However, the lower interface density also gives rise to lower incoherent phonon scattering and overall higher thermal conductivities.

3.4. Degree of randomness

RMLs with the same average period and composition ratio can still have different distributions of layer thickness within them. Since the interface densities and hence the degree of incoherent phonon scattering in such RMLs are the same, the variation in thermal conductivity at a particular average period, observed in Fig. 3 (a), is attributed to varying degrees of localization of coherent phonon modes within the RMLs. The existence of partially localized phonon modes in RMLs was identified from the thermal conductivity accumulation with respect to phonon frequency by Juntunen et al. [34]. Such partially localized modes, which have finite contribution to thermal conductivity of RMLs, will depend on the local randomization of layers throughout the RML structure. The degree of randomization of a RML can be quantified by the normalized average deviation of layer thicknesses from that of the corresponding SL of the same period, and is given by

$$DOR = \frac{\sum_{i=1}^{n}|t_i - \bar{d}/2|}{n \times \bar{d}/2} \tag{3}$$

Here, n is the number of periods in the RML, t_i is the thickness of individual layers and $\bar{d}$ is the average RML period which is also the corresponding SL period. Normalization by the mean period accounts for the fact that the same average deviation from a smaller mean period causes a larger degree of randomness than from a larger mean period. The variation of thermal conductivity with *DOR* is plotted in Fig. 5 (a) for all RML structures with an average period of $\bar{d} = \bar{d}_{min,RML} = 1.85$ nm and a composition ratio of 1. Although it is intuitively expected that a

larger deviation from the periodic SL structure leads to lower thermal conductivity of RMLs, we surprisingly find that the RML structure with minimum thermal conductivity occurs at an intermediate degree of randomness. Moreover, a variation in thermal conductivity of 25% is observed within structures at this degree of randomness. To understand the reasons governing this non-intuitive trend, we calculate the thermal boundary resistance (TBR) at the interfaces within four RMLs selected at different degrees of randomness, as marked in Fig. 5. To eliminate the effect of lattice mismatch, the lattice constants of both Si and Ge in these simulations are fixed at 0.543 nm. The trends in thermal conductivity obtained for these lattice-matched RMLs is verified to be similar to those in the original systems. The TBRs obtained within the four structures are shown in Fig. 5(b–e), superimposed on the corresponding RML structures for easier visualization. At low values of DOR, the deviation of the RML from the corresponding SL is low and much of it retains the periodic structure. As a result, localization of coherent phonons is less in these RMLs, leading to coupled interfaces with low values of TBR in these periodic regions as seen in Fig. 5 (d). On the other hand, high values of DOR require some layer thicknesses of the RML to be quite large, while other regions are necessarily composed of contiguous single layers leading to periodic interfaces and low TBR values (Fig. 5 (e)). However, at an intermediate degree of randomness, the occurrence of both small and large layer thicknesses interspersed among each other creates a favourable environment for coherent phonon localization, leading to relatively higher values of TBR across the entire structure (Fig. 5 (b)). Finally, Fig. 5 (c) shows the TBRs calculated in another RML at this intermediate DOR, in which periodic sections with low interfacial resistances are noticed. Although the distribution of layer thicknesses in this RML are similar to the best structure (b), the different relative placement of these layers within the RML leads to formation of periodic zones within this RML with low interfacial resistances and higher thermal conductivity.

4. Conclusions

To summarize, we have searched for the lower limit of thermal conductivity in Si/Ge based RML systems using both an intuition-guided manual search and a genetic algorithm based search process. We find that our manual search is, at best, able to converge to a local minimum of thermal conductivity, while the machine-learning based search can efficiently lead us toward the RML structure with the globally minimum thermal conductivity. The minimum RML thermal conductivity is found to occur at an average RML period that is much lower than the period of minimum SL thermal conductivity. The location of this average period is determined by a tradeoff between high interface density at smaller periods and sufficient scope for randomizing the layer thicknesses at larger periods. The variation in thermal conductivity within RMLs having the same period is further resolved by defining the degree of randomness as a measure of deviation of the RML layer thicknesses from the periodic SL layer thickness. We have shown that the GA optimized minimum thermal conductivity occurs for RMLs with an intermediate degree of randomness. By calculating the thermal boundary resistances within different RMLs, it is observed that greater local mismatch between adjacent layers leads to higher coherent phonon localization and thus higher TBRs. The different distributions of layer thickness and moreover the spatial placement of these layers causes a variation in the degree of coherent phonon localization. The generality of our optimization method implies that it can be applied to other systems as well such as graphene sheets with disordered arrangement of pores and binary superlattices with rough interfaces of different geometries. Finally, we would like to mention that our observed trends in thermal conductivity of RML systems are governed by general phonon transport properties such as phonon wavelengths, mean free paths and coherence lengths. Although we investigate the Si/Ge based RML system in this work, the non-intuitive trends in the variation of RML thermal conductivity with respect to the different structural parameters should be easily applicable to other RML systems as well such as conceptual Lennard-Jones
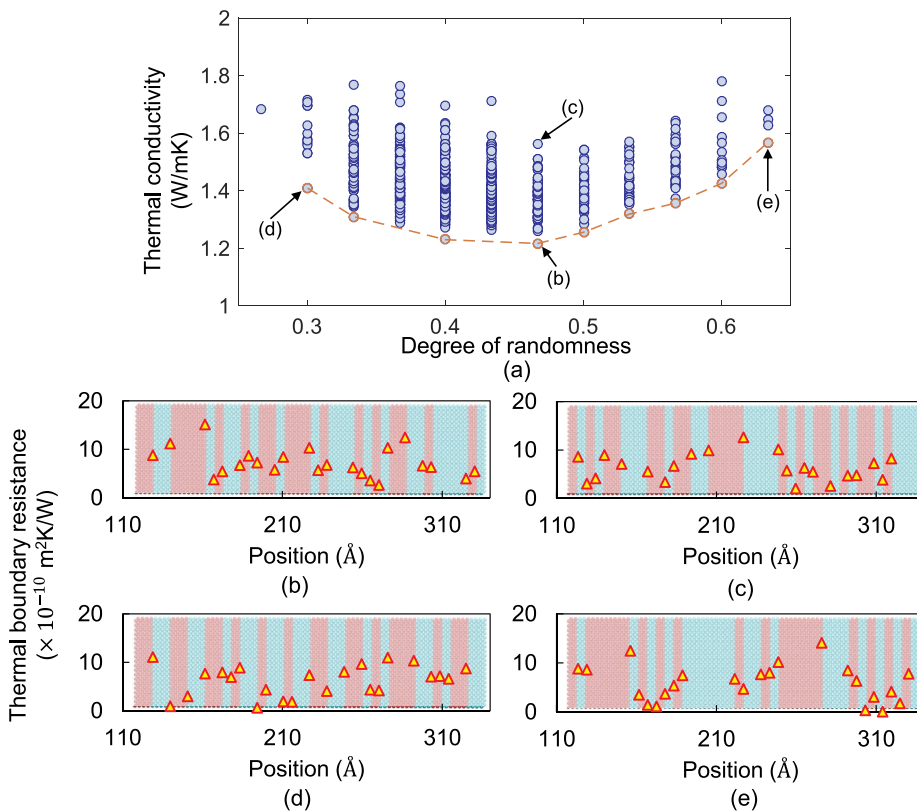

Fig. 5. (a) Dependence of thermal conductivity of RML structures on the degree of randomness (DOR) as defined in the text. The orange circles and dashed lines represent the lower bound of thermal conductivity obtained using our machine-learning based search process. For the four structures marked in the plot, the calculated thermal boundary resistances of all interfaces in each of the structures, superimposed on the visualization of the RML structures themselves, are shown in figures (b)–(e).

materials as well as more practical Bi_2Te_3/Sb_2Te_3 or GaAs/AlAs systems.

Declaration of competing interest

The authors declare that they have no known competing financial interests or personal relationships that could have appeared to influence the work reported in this paper.

Acknowledgements

References

[1] A.L. Moore, L. Shi, Emerging challenges and materials for thermal management of electronics, Mater. Today 17 (4) (2014) 163–174.

[2] P. Goli, S. Legedza, A. Dhar, R. Salgado, J. Renteria, A.A. Balandin, Graphene-enhanced hybrid phase change materials for thermal management of li-ion batteries, J. Power Sources 248 (2014) 37–43.

[3] R. Prasher, Thermal interface materials: historical perspective, status, and future directions, Proc. IEEE 94 (8) (2006) 1571–1586, https://doi.org/10.1109/JPROC.2006.879796.

[4] K.M. Shahil, A.A. Balandin, Graphene–multilayer graphene nanocomposites as highly efficient thermal interface materials, Nano Lett. 12 (2) (2012) 861–867.

[5] D. Clarke, C. Levi, Materials design for the next generation thermal barrier coatings, Annu. Rev. Mater. Res. 33 (1) (2003) 383–417.

[6] D.R. Clarke, S.R. Phillpot, Thermal barrier coating materials, Mater. Today 8 (6) (2005) 22–29.

[7] T. Feng, X. Ruan, Prediction of spectral phonon mean free path and thermal conductivity with applications to thermoelectrics and thermal management: a review, J. Nanomater. 2014 (2014).

[8] L. Lindsay, D.A. Broido, T.L. Reinecke, Phonon-isotope scattering and thermal conductivity in materials with a large isotope effect: a first-principles study, Phys. Rev. B 88 (2013), 144306, https://doi.org/10.1103/PhysRevB.88.144306.

[9] J. Hu, S. Schiffli, A. Vallabhaneni, X. Ruan, Y.P. Chen, Tuning the thermal conductivity of graphene nanoribbons by edge passivation and isotope engineering: a molecular dynamics study, Appl. Phys. Lett. 97 (13) (2010), 133107.

[10] N. Burger, A. Laachachi, M. Ferriol, M. Lutz, V. Toniazzo, D. Ruch, Review of thermal conductivity in composites: mechanisms, parameters and theory, Prog. Polym. Sci. 61 (2016) 1–28.

[11] T. Feng, X. Ruan, Z. Ye, B. Cao, Spectral phonon mean free path and thermal conductivity accumulation in defected graphene: the effects of defect type and concentration, Phys. Rev. B 91 (22) (2015) 224301.

[12] D. Medlin, G. Snyder, Interfaces in bulk thermoelectric materials: a review for current opinion in colloid and interface science, Curr. Opin. Colloid Interface Sci. 14 (4) (2009) 226–235.

[13] R. Venkatasubramanian, Lattice thermal conductivity reduction and phonon localization like behavior in superlattice structures, Phys. Rev. B 61 (2000) 3091–3097, https://doi.org/10.1103/PhysRevB.61.3091.

[14] R. Venkatasubramanian, E. Siivola, T. Colpitts, B. O'quinn, Thin-film thermoelectric devices with high room-temperature figures of merit, Nature 413 (6856) (2001) 597.

[15] H. Böttner, G. Chen, R. Venkatasubramanian, Aspects of thin-film superlattice thermoelectric materials, devices, and applications, MRS Bull. 31 (3) (2006) 211–217.

[16] I. Chowdhury, R. Prasher, K. Lofgreen, G. Chrysler, S. Narasimhan, R. Mahajan, D. Koester, R. Alley, R. Venkatasubramanian, On-chip cooling by superlattice-based thin-film thermoelectrics, Nat. Nanotechnol. 4 (4) (2009) 235.

[17] M.V. Simkin, G.D. Mahan, Minimum thermal conductivity of superlattices, Phys. Rev. Lett. 84 (2000) 927–930, https://doi.org/10.1103/PhysRevLett.84.927.

[18] B.C. Daly, H.J. Maris, K. Imamura, S. Tamura, Molecular dynamics calculation of the thermal conductivity of superlattices, Phys. Rev. B 66 (2002), 024301, https://doi.org/10.1103/PhysRevB.66.024301.

[19] Y. Chen, D. Li, J.R. Lukes, Z. Ni, M. Chen, Minimum superlattice thermal conductivity from molecular dynamics, Phys. Rev. B 72 (17) (2005), 174302.

[20] H. Mizuno, S. Mossa, J.-L. Barrat, Beating the amorphous limit in thermal conductivity by superlattices design, Sci. Rep. 5 (2015) 14116.

[21] K. Termentzidis, P. Chantrenne, J.-Y. Duquesne, A. Saci, Thermal conductivity of gaas/alas superlattices and the puzzle of interfaces, J. Phys. Condens. Matter 22 (47) (2010), 475001.

[22] T. Borca-Tasciuc, W. Liu, J. Liu, T. Zeng, D.W. Song, C.D. Moore, G. Chen, K. L. Wang, M.S. Goorsky, T. Radetic, et al., Thermal conductivity of symmetrically strained si/ge superlattices, Superlattice Microstruct. 28 (3) (2000) 199–206.

[23] B. Saha, Y.R. Koh, J. Comparan, S. Sadasivam, J.L. Schroeder, M. Garbrecht, A. Mohammed, J. Birch, T. Fisher, A. Shakouri, et al., Cross-plane thermal conductivity of (ti,w) n/(al, sc) n metal/semiconductor superlattices, Phys. Rev. B 93 (4) (2016), 045311.

[24] S. Chakraborty, C. Kleint, A. Heinrich, C. Schneider, J. Schumann, M. Falke, S. Teichert, Thermal conductivity in strain symmetrized si/ge superlattices on si (111), Appl. Phys. Lett. 83 (20) (2003) 4184–4186.

[25] J. Caylor, K. Coonley, J. Stuart, T. Colpitts, R. Venkatasubramanian, Enhanced thermoelectric performance in pbte-based superlattice structures from reduction of lattice thermal conductivity, Appl. Phys. Lett. 87 (2) (2005), 023105.

[26] A. Frachioni, B. White Jr., Simulated thermal conductivity of silicon-based random multilayer thin films, J. Appl. Phys. 112 (1) (2012), 014320.

[27] Y. Wang, H. Huang, X. Ruan, Decomposition of coherent and incoherent phonon conduction in superlattices and random multilayers, Phys. Rev. B 90 (2014) 165406, https://doi.org/10.1103/PhysRevB.90.165406.

[28] Y. Wang, C. Gu, X. Ruan, Optimization of the random multilayer structure to break the random-alloy limit of thermal conductivity, Appl. Phys. Lett. 106 (7) (2015), 073104.

[29] X. Mu, L. Wang, X. Yang, P. Zhang, A.C. To, T. Luo, Ultra-low thermal conductivity in si/ge hierarchical superlattice nanowire, Sci. Rep. 5 (2015) 16697.

[30] B. Qiu, G. Chen, Z. Tian, Effects of aperiodicity and roughness on coherent heat conduction in superlattices, Nanoscale Microscale Thermophys. Eng. 19 (4) (2015) 272–278.

[31] P. Chakraborty, L. Cao, Y. Wang, Ultralow lattice thermal conductivity of the random multilayer structure with lattice imperfections, Sci. Rep. 7 (1) (2017) 8134.

[32] R. Frieling, S. Eon, D. Wolf, H. Bracht, Molecular dynamics simulations of thermal transport in isotopically modulated semiconductor nanostructures, Phys. Status Solidi 213 (3) (2016) 549–556.

[33] S. Hu, Z. Zhang, P. Jiang, J. Chen, S. Volz, M. Nomura, B. Li, Randomness-induced phonon localization in graphene heat conduction, J. Phys. Chem. Lett. 9 (14) (2018) 3959–3968.

[34] T. Juntunen, O. Vänskä, I. Tittonen, Anderson localization quenches thermal transport in aperiodic superlattices, Phys. Rev. Lett. 122 (2019) 105901, https://doi.org/10.1103/PhysRevLett.122.105901.

[35] S. Ju, T. Shiga, L. Feng, Z. Hou, K. Tsuda, J. Shiomi, Designing nanostructures for phonon transport via bayesian optimization, Phys. Rev. X 7 (2017), 021024, https://doi.org/10.1103/PhysRevX.7.021024.

[36] A. Seko, A. Togo, H. Hayashi, K. Tsuda, L. Chaput, I. Tanaka, Prediction of low-thermal-conductivity compounds with first-principles anharmonic lattice-dynamics calculations and bayesian optimization, Phys. Rev. Lett. 115 (2015), 205901, https://doi.org/10.1103/PhysRevLett.115.205901.

[37] T.M. Dieb, S. Ju, K. Yoshizoe, Z. Hou, J. Shiomi, K. Tsuda, Mdts: automatic complex materials design using Monte Carlo tree search, Sci. Technol. Adv. Mater. 18 (1) (2017) 498–503.

[38] A.R. Oganov, C.W. Glass, Crystal structure prediction using ab initio evolutionary techniques: principles and applications, J. Chem. Phys. 124 (24) (2006) 244704.

[39] T.M. Dieb, Z. Hou, K. Tsuda, Structure prediction of boron-doped graphene by machine learning, J. Chem. Phys. 148 (24) (2018), 241716.

[40] H. Zhang, A.J. Minnich, The best nanoparticle size distribution for minimum thermal conductivity, Sci. Rep. 5 (2015) 8995.

[41] M. Yamawaki, M. Ohnishi, S. Ju, J. Shiomi, Multifunctional structural design of graphene thermoelectrics by bayesian optimization, Science Advances 4 (6) (2018) eaar4192.

[42] N.P. Jouppi, C. Young, N. Patil, D. Patterson, G. Agrawal, R. Bajwa, S. Bates, S. Bhatia, N. Boden, A. Borchers, et al., In-datacenter performance analysis of a tensor processing unit, in: 2017 ACM/IEEE 44th Annual International Symposium on Computer Architecture (ISCA), IEEE, 2017, pp. 1–12.

[43] S. Wen, X. Xie, Z. Yan, T. Huang, Z. Zeng, General memristor with applications in multilayer neural networks, Neural Netw. 103 (2018) 142–149.

[44] S. Sen, S. Venkataramani, A. Raghunathan, Approximate computing for spiking neural networks, in: Design, Automation & Test in Europe Conference & Exhibition (DATE), 2017, IEEE, 2017, pp. 193–198.

[45] C. Aporntewan, P. Chongstitvatana, A hardware implementation of the compact genetic algorithm, in: Proceedings of the 2001 Congress on Evolutionary Computation (IEEE Cat. No. 01TH8546), vol. 1, IEEE, 2001, pp. 624–629.

[46] S. Wakabayashi, T. Koide, K. Hatta, Y. Nakayama, M. Goto, N. Toshine, Gaa: a vlsi genetic algorithm accelerator with on-the-fly adaptation of crossover operators, in: ISCAS'98. Proceedings of the 1998 IEEE International Symposium on Circuits and Systems (Cat. No. 98CH36187), vol. 2, IEEE, 1998, pp. 268–271.

[47] K. Irick, M. DeBole, V. Narayanan, A. Gayasen, A hardware efficient support vector machine architecture for fpga, in: 2008 16th International Symposium on Field-Programmable Custom Computing Machines, IEEE, 2008, pp. 304–305.

[48] J. Garg, N. Bonini, B. Kozinsky, N. Marzari, Role of disorder and anharmonicity in the thermal conductivity of silicon-germanium alloys: a first-principles study, Phys. Rev. Lett. 106 (2011), 045901, https://doi.org/10.1103/PhysRevLett.106.045901.

[49] T. Hori, T. Shiga, J. Shiomi, Phonon transport analysis of silicon germanium alloys using molecular dynamics simulations, J. Appl. Phys. 113 (20) (2013), 203514.

[50] S.-i. Tamura, Y. Tanaka, H.J. Maris, Phonon group velocity and thermal conduction in superlattices, Phys. Rev. B 60 (1999) 2627–2630, https://doi.org/10.1103/PhysRevB.60.2627.

[51] S. Volz, J. Saulnier, G. Chen, P. Beauchamp, Computation of thermal conductivity of si/ge superlattices by molecular dynamics techniques, Microelectron. J. 31 (9–10) (2000) 815–819.

[52] E.S. Landry, A.J.H. McGaughey, Effect of interfacial species mixing on phonon transport in semiconductor superlattices, Phys. Rev. B 79 (2009), 075316, https://doi.org/10.1103/PhysRevB.79.075316.

[53] Y. Chalopin, K. Esfarjani, A. Henry, S. Volz, G. Chen, Thermal interface conductance in si/ge superlattices by equilibrium molecular dynamics, Phys. Rev. B 85 (2012) 195302, https://doi.org/10.1103/PhysRevB.85.195302.

[54] C. Dames, G. Chen, Theoretical phonon thermal conductivity of si/ge superlattice nanowires, J. Appl. Phys. 95 (2) (2004) 682–693.

[55] M. Hu, K.P. Giapis, J.V. Goicochea, X. Zhang, D. Poulikakos, Significant reduction of thermal conductivity in si/ge core- shell nanowires, Nano Lett. 11 (2) (2010) 618–623.

[56] M. Hu, D. Poulikakos, Si/ge superlattice nanowires with ultralow thermal conductivity, Nano Lett. 12 (11) (2012) 5487–5494.

[57] S. Plimpton, Fast parallel algorithms for short-range molecular dynamics, J. Comput. Phys. 117 (1) (1995) 1–19.

[58] J. Tersoff, Modeling solid-state chemistry: interatomic potentials for multicomponent systems, Phys. Rev. B 39 (1989) 5566–5568, https://doi.org/10.1103/PhysRevB.39.5566.

Prabudhya is a Ph.D. student at Purdue University, and his current research interest is in thermal transport in thermo-electric nanomaterials. He received his B.S. and M.S. from the Indian Institute of Technology, Kharagpur in 2016.

Colleen Reynolds received her bachelors and masters in Materials Science and Engineering from the University of Pennsylvania in 2014. She then worked at Lockheed Martin's Advanced Technology Laboratories as a research scientist until 2018. Colleen is currently pursuing a PhD at the University of California at Santa Barbara Materials Department working under Professors Anton Van der Ven and Tresa Pollock where her research is focused on refractory multi-principle element alloys.
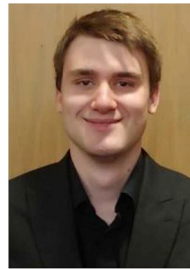
Adam Garrett is a senior student in the School of Mechanical Engineering at Purdue University. He will be continuing on to get his Master's in Mechanical Engineering starting Fall 2020 in the field of thermal and fluid sciences.

Dr. Tianli Feng is a postdoctoral fellow at Oak Ridge National Laboratory. He received his B.S. in Physics at the University of Science and Technology of China in 2011. He received his M.S. and Ph.D. in Mechanical Engineering at Purdue University in 2013 and 2017, respectively. His research interests are in multiscale simulations and data sciences-enabled engineering of energy transport, conversion and storage.

Shashishekar P. Adiga obtained his Ph.D. in Materials Science and Engineering at North Carolina State University in 2003. He currently heads the Materials and Simulations team at Samsung Advanced Institute of Technology (SAIT), India in Bangalore. Prior to joining SAIT, Adiga worked at Argonne National Laboratory, Kodak Research Labs, Lockheed Martin Advanced Technology Laboratories and Shell Technology Center. His research interests include computational materials science, materials for energy storage and conversion, automated materials discovery, functional and device materials. He has over 30 publications, and several patents.

Dr. Xiulin Ruan is a professor in the School of Mechanical Engineering and the Birck Nanotechnology Center at Purdue University. He received his B.S. and M.S. in Engineering Thermophysics from Tsinghua University in 2000 and 2002, respectively. He received an M.S. in Electrical Engineering and Ph.D. in Mechanical Engineering from the University of Michigan at Ann Arbor, in 2006 and 2007 respectively. His research interests are in multiscale multiphysics simulations and experiments of phonon, electron, and photon transport and interactions, for various emerging applications.